

On the relationship between Potential Vorticity and Cyclogenesis

A. K AL-Khalaf

Department of Meteorology, Faculty of Meteorology, Environment, and Arid Land Agriculture, King Abdulaziz University, Jeddah, Saudi Arabia.

ABSTRACT

Cyclones and anticyclones are the dominant synoptic scale meteorological weather systems in midlatitudes. An attractive way to study dynamical aspects of these structures is provided by the use of potential vorticity (PV) framework. In this paper several aspects of midlatitude cyclogenesis are investigated within this PV framework using a case study analyses. The analysis of absolute, relative and potential vorticity imply the significance of the upper level dynamics in the initiation of this case of cyclogenesis. On one hand, the isobaric vorticity analysis appears to be an informative, accurate and easy to use as a method for describing the upper-level dynamics. On the other hand the PV analysis provided a summarized picture of the development and the evolution at upper and lower levels, which is directly visible, on the basis of a smaller number of plots compared with the isobaric vorticity analysis. The display of the time sequence of the PV on the appropriate isentropic surface helped in easily understanding the dynamics of the three-dimensional upper level development.

1. Introduction

In recent years, cyclogenesis over the central Mediterranean region has become the subject of considerable research (Prezerakos, 1991,1992; Prezerakos et al. 1999; Karacostas and Flocas, 1983; Flocas and Karacostas, 1996), since these synoptic-scale events cause intense winds, precipitation and temperature drop. Because of the intimate connection between the phenomena and local weather prediction, interest in understanding the characteristics of cyclogenesis over this region is enormous and ongoing.

On the other hand, in the last decade, great emphasis has been placed on the analysis of the isentropic potential vorticity. Although, this dynamic atmospheric parameter was introduced in the 1940's by Rossby (1940) and Ertel (1942), its application in meteorological research was limited, mainly because of the complexity of its calculation. Since Hoskins et al. (1985) acknowledged the analysis of isentropic potential vorticity as a very important diagnostic tool to understand the mechanisms responsible for atmospheric development better; the interest of the research community has increased

enormously in this topic.

According to Hoskins et al. (1985), the potential vorticity analysis on isentropic surface summarizes the combined effect of the vorticity and temperature advection and allows the estimation of the vertical motion. The objective of the present work is to diagnose our case of study in the context of absolute, relative and potential vorticity analysis in order to examine in detail the key dynamical aspects of the cyclonic development.

2. Data and methodology

The data used in this study have been taken from the archives of the European Center for Medium-Range Weather Forecasts (ECMWF). It consists of the horizontal wind components (u - eastward, v -northward), the temperature (T) and the geopotential height (z) on regular latitude-longitude grid points resolution of $2.5^\circ \times 2.5^\circ$ for the isobaric levels 1000, 850, 700, 500, 300, 200 and 100 hPa. The data used is only at 1200 GMT during the period 17 to 28 January 2005. The domain of study extends from 10° W to 60° E and from 10° N to 70° N. The inner domain which is used for the present study changes with time to enclose the cyclone during its life cycle (Fig. 2).

Centered finite differences were used to compute horizontal derivatives and all vertical derivatives except those at the 1000 and 100 hPa, where non-centered differences were employed. The vertical motion, ω , is computed using the Q-vector representation of the quasi-geostrophic ω equation by using the relaxation method (Krishnamurti and Bounoua, 1996). The relative vorticity and absolute vorticity advection have been calculated from the actual data using the central finite differences method.

It is well known (Petterssen; 1956; Palmén and Newton, 1969; Carlson, 1991) that the isobaric absolute vorticity together with their respective advections, are effective diagnostic tools for studying the development of synoptic-scale extratropical atmospheric circulation systems. The local rate of change of relative vorticity is derived from the simplified vorticity equation (Holton, 1979; Wiin-Nielsen 1973; Carlson, 1991):

$$\frac{\partial \zeta}{\partial t} = -\mathbf{V} \cdot \nabla_p (\zeta + f) - f_0 \nabla_p \cdot \mathbf{V} \quad (1)$$

Where, \mathbf{V} is the horizontal wind velocity, $f = f_0 + df / dy$ is the Coriolis parameter, with f_0 being the Coriolis parameter at reference latitude φ_0 and y the longitudinal distance, ∇_p is the horizontal gradient operator applied with pressure held constant, $\zeta =$

$k \cdot \nabla \times \mathbf{V}$ is the vertical component of relative vorticity. In equation (1), the first right-hand term is the horizontal advection of absolute vorticity and the second is the divergence term. This equation could be replaced by the quasi-geostrophic vorticity equation. The increase in relative vorticity near the surface depends mainly on the convergence term (development term), in the middle troposphere on the advection term, since convergence is almost zero (level of non divergence), while near the tropopause both terms are significant.

2.1 Estimation of potential vorticity

A principal indicator of a fold like ingress of stratospheric air into the troposphere is the occurrence of an anomalous high potential vorticity value reaching down towards middle tropospheric height levels. Hence, potential vorticity fields were calculated from the available meteorological parameters, namely temperature and the horizontal wind components on constant pressure surface. In isobaric coordinates the potential vorticity was approximated by the product of the vertical components of absolute vorticity and potential temperature gradients as

$$(\text{PV})_{\theta} = \left[\left(\frac{\partial v}{\partial x} - \frac{\partial u}{\partial y} \right) + f + \frac{R}{\sigma P} \left(\frac{\partial v}{\partial p} \frac{\partial T}{\partial x} - \frac{\partial u}{\partial p} \frac{\partial T}{\partial y} \right) \right] \frac{\partial \theta}{\partial p} \quad (2)$$

Where f is the coriolis parameter, θ is the potential temperature u the wind in x-direction of the grid (W-E in principle) and v the wind in y-direction.

Following WMO (1986) the dynamic tropopause is defined by the potential vorticity with $P = 1.6 \times 10^{-7} \text{ Kpa}^{-1} \text{ s}^{-1} = 1.6 \text{ PVU}$, where, for convenience, the potential vorticity unit (PVU) is defined to be $\times 10^{-7} \text{ Kpa}^{-1} \text{ s}^{-1}$.

3. Synoptic discussion

A common case of winter cyclogenesis over the Mediterranean is considered in the present study. Its period extended from 18 to 26 January 2005. Based on 1000 hPa and 500 hPa charts the life cycle of this cyclone can be divided into two periods. The first period (growth period) is from 18 to 23 January while the second period (decay period) is from 24 to 26 January. 1000 hPa and 500 hPa charts at 1200 GMT on each day are shown in Figs 1 and 2 respectively. 1000 hPa charts depict contours of height with 20

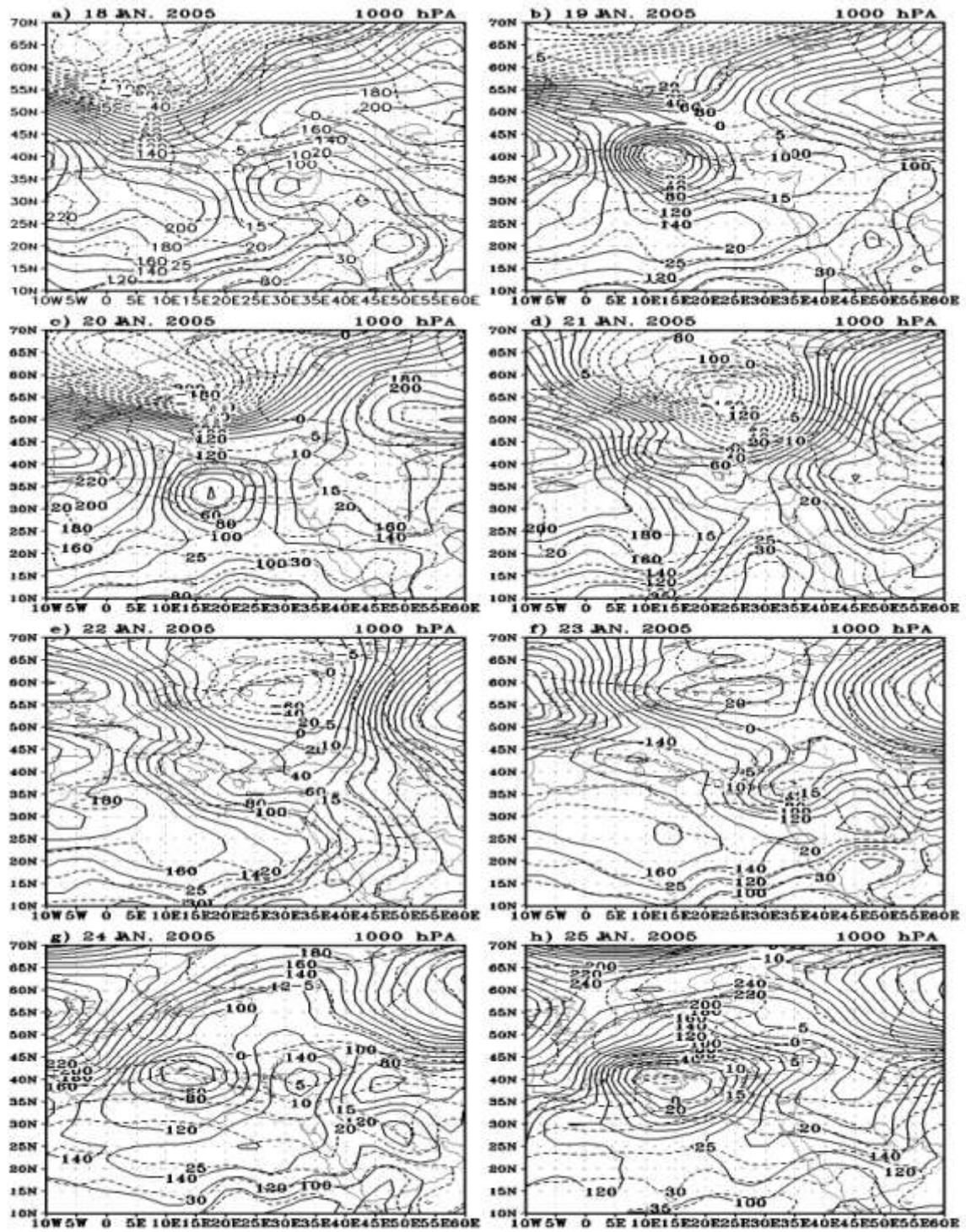


Fig. 1: 1000 hPa geopotential contour every 20 m intervals (solid) and temperature (dashed) every 5° C for 1200 UTC 18-25 January 2005.

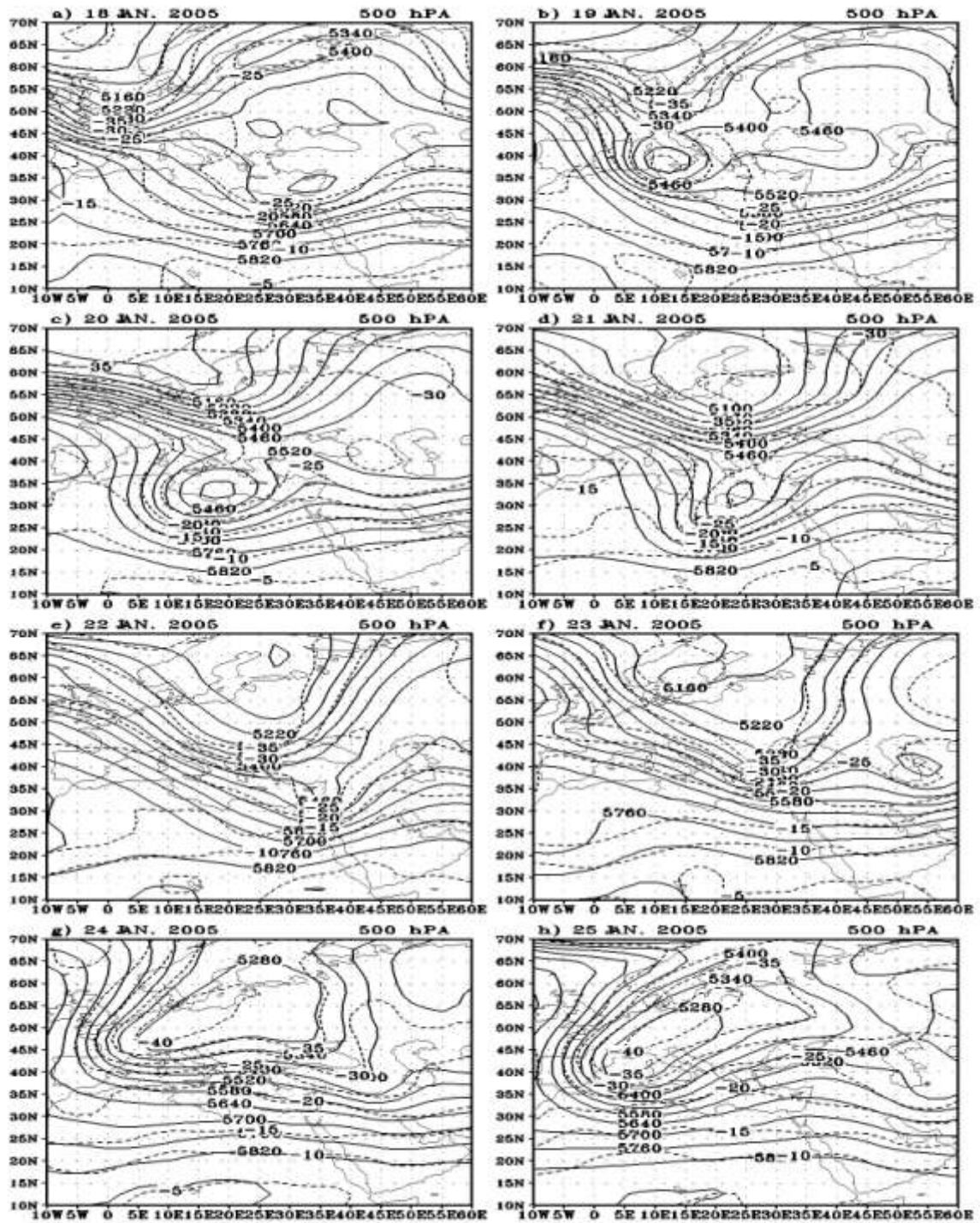


Fig. 2: 500 hPa geopotential contours every 40 m intervals (solid) and isotherms (dashed) every 5° C for 1200 UTC 18-25 January 2005.

geopotential meter (GPM) increment while upper air charts (500 hPa) contain contours of height with 40 GPM increment. The isotherms in the charts of the two levels are analyzed with 5° C increment. The cyclone of special interest first appeared as an extension of the traveling depression north west of Europe at 18 January. A cut-off low is formed at 19 January and a well-defined cyclonic depression become clear over south west of Italy. At 19 January a strong thermal gradient lies along the northern Italy and middle of Europe. In this highly baroclinic zone the surface storm undergoes strong intensification.

The evolution of the lee cyclogenesis was consistent at least in the second and third days, with the schematic processes outlined in Buzzi and Tibalidi (1978). The interaction of the cold front with the Alps produced the initial disturbances which then grow as a baroclinic disturbances.

During the next 24 hours, the the center of the low propagates slowly to the southeastward and the geopotential height at the center reaches to 20GPM (Figure 2c). A corresponding cut off low at 500 hPa becomes over north libya with center of 5400 GPM. On 21 January a strong development occurs at the surface and at the upper air, where the surface cyclone moved east ward and becomes continued (joins) with the main cyclone (its center at 55° N, 25° E). Also the inverted v-shap trough of the sudan low oscillate north ward to the north of the red sea and in the upper air (500 hPa) the cut of low also moved east ward to a point just north east of Egypt. At 1200 GMT 22 January (the rainy day), a strong interaction occurs between the trough that extended from the tropical region and that extended from middle latitude region, and the two cyclones becomes joints with other. The most interesting features is that there is north ward strong warm advection from the tropical region associated with the air flow around the sudan low and a south wad strong cold advection. The interaction between these two air masses causing a strong instability over the east of Mediterranean and at the west of saudia arabia. By 1200 GMT January, the trough of sudan low moved south west ward with the trough of the midllatitude low moved east ward to centered over Iran. During the next two days (25 and 26 January) the depression started filling and its central pressure increased gradually. On the other hand the high pressure over Atlantic is extended with a major ridge that joints the Siberian high on 22 January, Figure 2d. In other wards no more cold advection is permitted from the to the cyclone. While the Siberian high pressure propagate westward the horizontal extension of the cyclone decrease and moved slowly eastward, and it become stationary vortex rotating

above the north east of Mediterranean. Finally the cyclone was drifted slowly north-eastward and was out of the computational domain by 27 January.

4 Isobaric vorticity analysis

It has been recognized that central Mediterranean and northern African cyclogenesis is usually forced by a variety of upper-level tropospheric features. While the lower tropospheric physical and dynamic processes follow (Karein, 1979; Prezerakos, 1992; Prezerakos et. al., 1992). This is associated with the theory of Helmholtz (Petterssen, 1956) that supports the controlling of the relation between the low level baroclinicity and the surface cyclogenesis by the upper level forcing. The upper air circulation features originating in northwest Europe that have been recognized as precursors of central and eastern Mediterranean cyclogenesis (Prezerakos, 1992) are as follow:

a) Strong and rapid cold advection toward the central Mediterranean in the upper troposphere, associated with the mobile jet streaks appearing upon the flanks of an omega shaped blocking anticyclone centered on the British Isles,

b) The formation of a dynamically unstable ridge on the eastern flank of the above mentioned blocking high,

c) The evolution of an upper diffluent trough, due to the asymmetrical flow between its western and eastern sides and

d) The upper tropospheric cold dome in connection with its contribution to surface cyclogenesis.

Therefore, the identification and investigation of the upper tropospheric features that led to surface cyclogenesis on 20, 21 and 22 January is the major importance for forecasting the event.

4.1 Genesis of the initial disturbance at the upper levels

It is known that the subtropical (polar) jet has its maximum speed around 200 hPa (300 hPa). So, we display the 300 and 200 hPa isotach fields in the following discussion to show the behavior of the polar and subtropical jets during the development of our case study. Figures 3 and 4 display the isotach (wind speed) at 300 and 200 hPa from 18 to 25 January 2005. They show the behavior of the subtropical and polar jets at 200 and 300 hPa levels during the life cycle of our cyclone.

At 18 January an omega-shaped blocking over Northeast Atlantic and west Europe dominated the large-scale upper tropospheric circulation with a strong Northwest-southeast jet stream on its eastern flank (Figure 3). Because of the warm advection in the region of the jet streak, the ridge propagated slowly northeastwards, resulting in the amplification of the long wave. On 18 January 2005 (Figure 3a) the wind direction over north Africa is zonal and the maximum speed of the subtropical jet is 65 m/s and is located over northeast of Africa (over Libya, Egypt and north Red sea), its value at 200 hPa is greater than 75 m/s. The polar jet extended from northwest England to southeast Spain and north of Italy with a maximum wind greater than 75 m/s at 300 hPa, its extension at 200 hPa has a maximum wind greater than 65 m/s.

As the polar jet streak is shifted eastward and moved southeastward it continuously advected cold air southward. Consequently, in the following twenty-four hours, as shown in figure 3c, the baroclinicity ahead of the ridge increases and the jet streak moves southward. The synoptic situation at 300 hPa on the following two days (Figure 3c and 3d) is particularly important for the subsequent development. On 19 January 2005, the subtropical jet moves slightly to eastward and its maximum center becomes greater than 65 m/s at 300 and 200 hPa and was located over Saudi Arabia. While the polar jet is shifted eastward and moved south eastward to amalgamate with the subtropical jet and its maximum value becomes greater than 70 m/s at 300 and more than 60 m/s at 200 hPa. At this time (20 January) the system becomes cut off at all the isobaric levels, associated with relative vorticity maximum of $10 \times 10^{-5} \text{ s}^{-1}$ at 500 hPa (figure 5) and $14 \times 10^{-5} \text{ s}^{-1}$ at 300 hPa (not shown), and increased baroclinicity at these levels. At the surface, a frontal surface low becomes very pronounced and located over Italy, a head of and parallel to the polar jet stream. Therefore, when this type of atmospheric circulation dominates at the upper levels, intense surface cyclogenesis over the central Mediterranean is likely to be initiated, of course under favourable low level conditions (Prezerakos, 1992).

On 20 January, the subtropical jet was shifted to the southeast. The front of the polar jet reaches north of Algeria and its jet maximum wind value is greater than 75 m/s at 300 and 200 hPa. The subtropical jet weakened at 300 hPa and became stronger at 200 hPa (>70 m/s) and moved eastward. The amalgamation between the two jets continues also at 21 January. Beginning with the day of 22 up to 25 January the polar jet weakened at 200

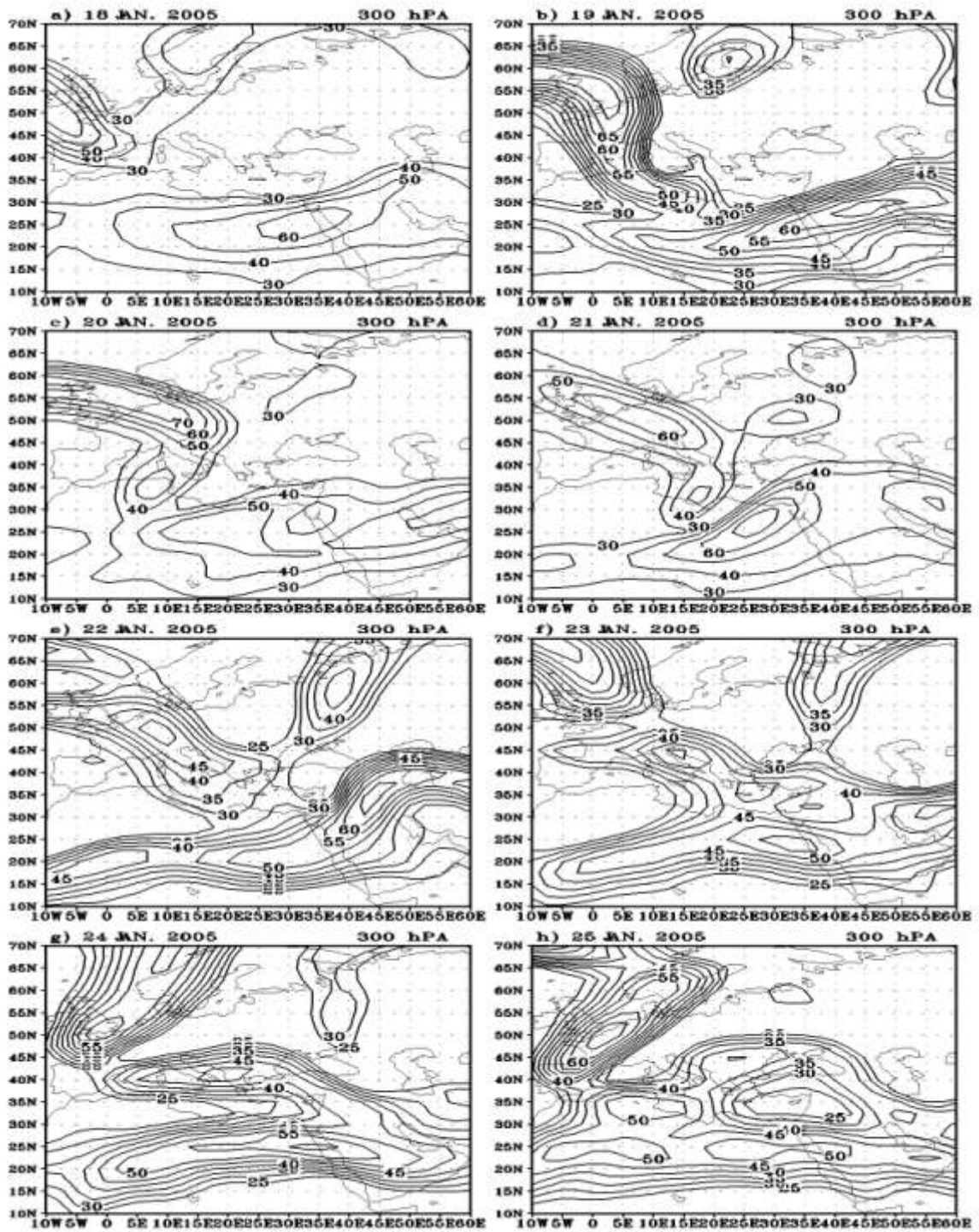


Fig. 3: Isotachs at 300 hPa, those ≥ 25 m/s, every 5m/s, for 1200 UTC 18-25 January 2005.

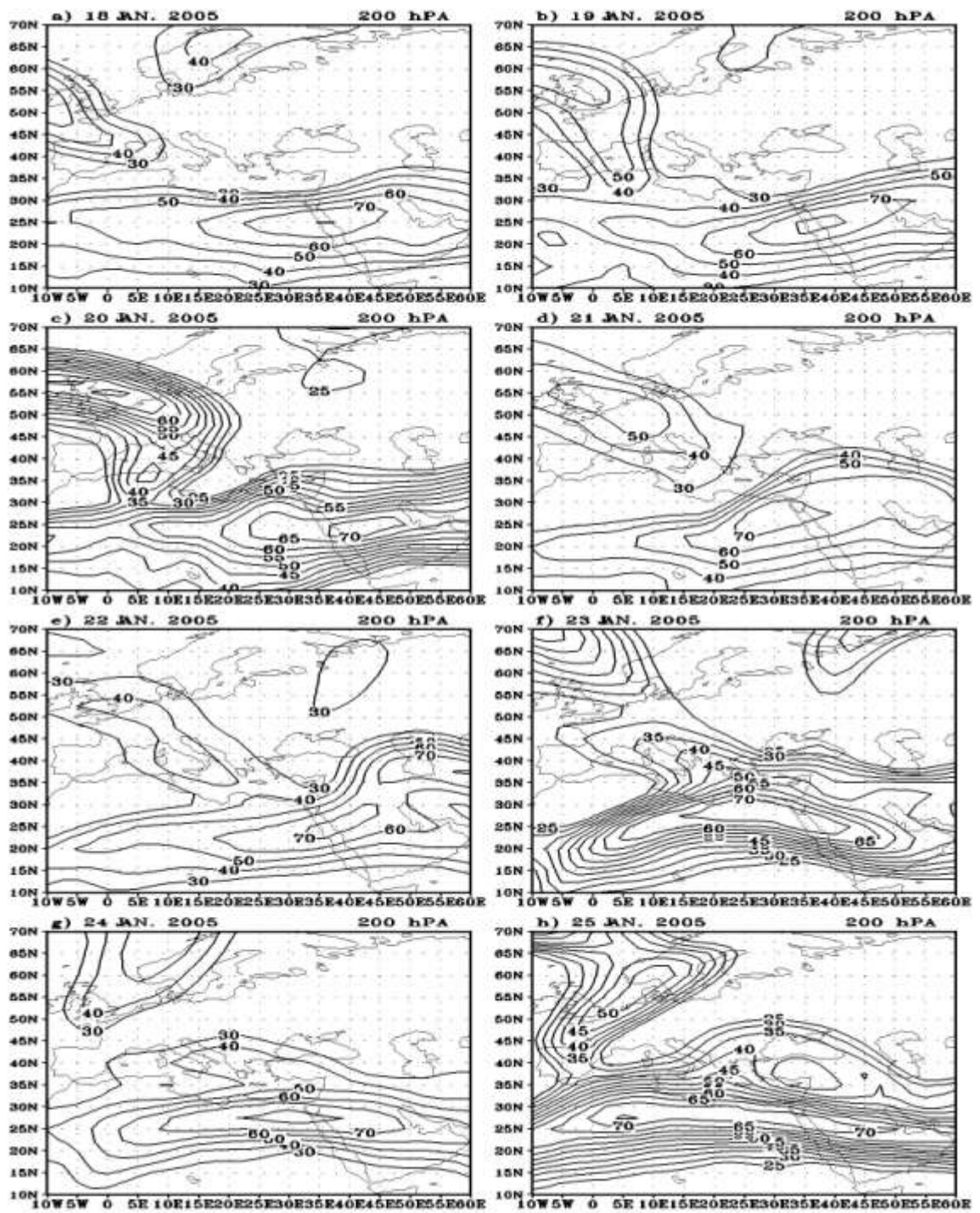


Fig. 4: Isotachs at 200 hPa, those ≥ 25 m/s, every 5m/s, for 1200 UTC 18-25 January 2005.

hPa and the amalgamation with the subtropical jet disappears. On 24 and 25 January the polar jet extended from north Europe to northwest Africa with a maximum wind greater than 65 m/s at 300 hPa.

During the last three days, we notice that the subtropical jet is moved westward and were almost back to the normal distribution in both speed and direction.

4.2 Initiation of the surface cyclogenesis

Figure 5 Shows the field of relative vorticity at 850 hPa during the period of study. It shows that the relative vorticity undergoes a rapid change of its magnitude, orientation and horizontal extension from day to day. At 18 January we have three cells of maximum relative vorticity, the first is located at (60° N, 7.5° W) while the other two cells are at (47° N, 2.5° E) and (32.5° N, 27.5° E). Here we are interest in the first and second cells, which represent and accompany the cyclone development. During the next 24 hours the second cell moved southeastward and its center is located at (40° N, 10° E), while the other two cells moved eastwards. By 20 January the first cell strenthing and moved southwestward (55° N, 15° E) while the second cell moved slowly southwest ward and is originated at (30° N, 15° E), the third cell disappeared. The maximum value of the relative vorticity of the second cell is $7 \times 10^{-5} \text{ s}^{-1}$ while it is greater than $9 \times 10^{-5} \text{ s}^{-1}$ for the first cell (figure 5). During the next 24 hours the first cell undergoes a rapid changes in its origination and magnitude, it is center moved about 10 logtude southeastward and its magnitude amounting to $8 \times 10^{-5} \text{ s}^{-1}$ at (55° N, 25° E). In the following 24 hours, this center moved rather slowly northeastward and its value decreased to $4 \times 10^{-5} \text{ s}^{-1}$, while the second one moved eastward to originat over north east of KSA . By 23 January the second cell strenthing and moved northwestward (37° N, 32.5° E) while the first cell moved slowly southwest ward and is originated at (57° N, 10° E). In the last two days (as the cyclone retarded west ward) the values of the center of relative vorticity decreases gradually to reach its minimum on the 25 January.

Figure 6 shows the relative vorticity at 500 hPa during the period of interest. Attention is focused on the center of maximum relative vorticity ($10 \times 10^{-5} \text{ s}^{-1}$) that found in the northwest corner of the domain figure 6a. After 24 hours this center is strengthen and moved southeastward, its value reached to $14 \times 10^{-5} \text{ s}^{-1}$. On 20 January this center moved southwestward and originated at (32.5° N, 15° E). By 21 January the maximum of

vorticity located at 25° N, 20° E moved eastward to reach east of Mediterranean at 22 January with a value of $10 \times 10^{-5} \text{ s}^{-1}$ over east of Mediterranean (Figure 6e). Figure 10f shows that the cell of positive relative vorticity occupies a large area of the domain, but the maximum decreases to $8 \times 10^{-5} \text{ s}^{-1}$. With the beginning of the last two days the cyclone retarded westward and the values of positive vorticity decreases and continues occupies a large area of the domain of study.

On 20 January (figure 3) shows that a synoptic-scale wave is present over NW Europe at the isobaric level of 500 hPa and its trough gets, with a NE-SW tilt. The jet wind maximum is 70 m s^{-1} at 300 hPa. The wind speed decreased along the jet stream axis from the west to the east side of the trough resulting in an increase of the mean absolute vorticity advection in its region (Palmen and Newton, 1969). Indeed, the left side region of the jet stream axis (polar jet) is characterized by positive advection of absolute vorticity with a maximum amounting to $(35 \times 10^{-10} \text{ s}^{-2})$ which was moving rapidly southwards. According to Petterssen (1956) and Kurz (1994), this synoptic situation is a precursor to development. In association with the absolute vorticity advection, Austria and Northern Italy were covered by a field of ascending motion at the isobaric level of 500 hPa, with the strongest ascent of 0.4 Pa s^{-1} laying over northwest Italy (figure 7c). The positive relative vorticity had increased to $10 \times 10^{-5} \text{ s}^{-1}$ over Libya by 21 January, while the east of Mediterranean is characterized by positive absolute vorticity advection, implying the deepening of the upper trough.

The maximum absolute vorticity advection, located at (30° N, 25° E) had intensified to $40 \times 10^{-10} \text{ s}^{-2}$, where the ascending motion becomes 0.3 Pa s^{-1} at 500 hPa (figure 7d). The relative humidity at 850 hPa was more than 90 % as shown in figure 7d. According to the 1000 hPa analysis figure 2d, the low-pressure center had developed over this area by 21 January, as the frontal zone had moved to the same region being under the maximum absolute vorticity advection (figure 5d). It is noteworthy that at the time of the surface cyclogenesis over central and eastern Mediterranean had intensified, the 300 hPa isotach analysis (figure 3d) suggests that the northerly polar frontal jet, curved cyclonically over central Mediterranean, tended to interact with the westerly subtropical jet that was propagated along the Libyan coast. By 21 January as the orientation of the trough axis at 500 hPa had changed from NE- SW to N- S, extensive cyclonic development is marked (Carlson, 1991) and the low center at 500 hPa tends to develop (figure 2d). The surface low-pressure system became circularly organized and it deepened significantly near

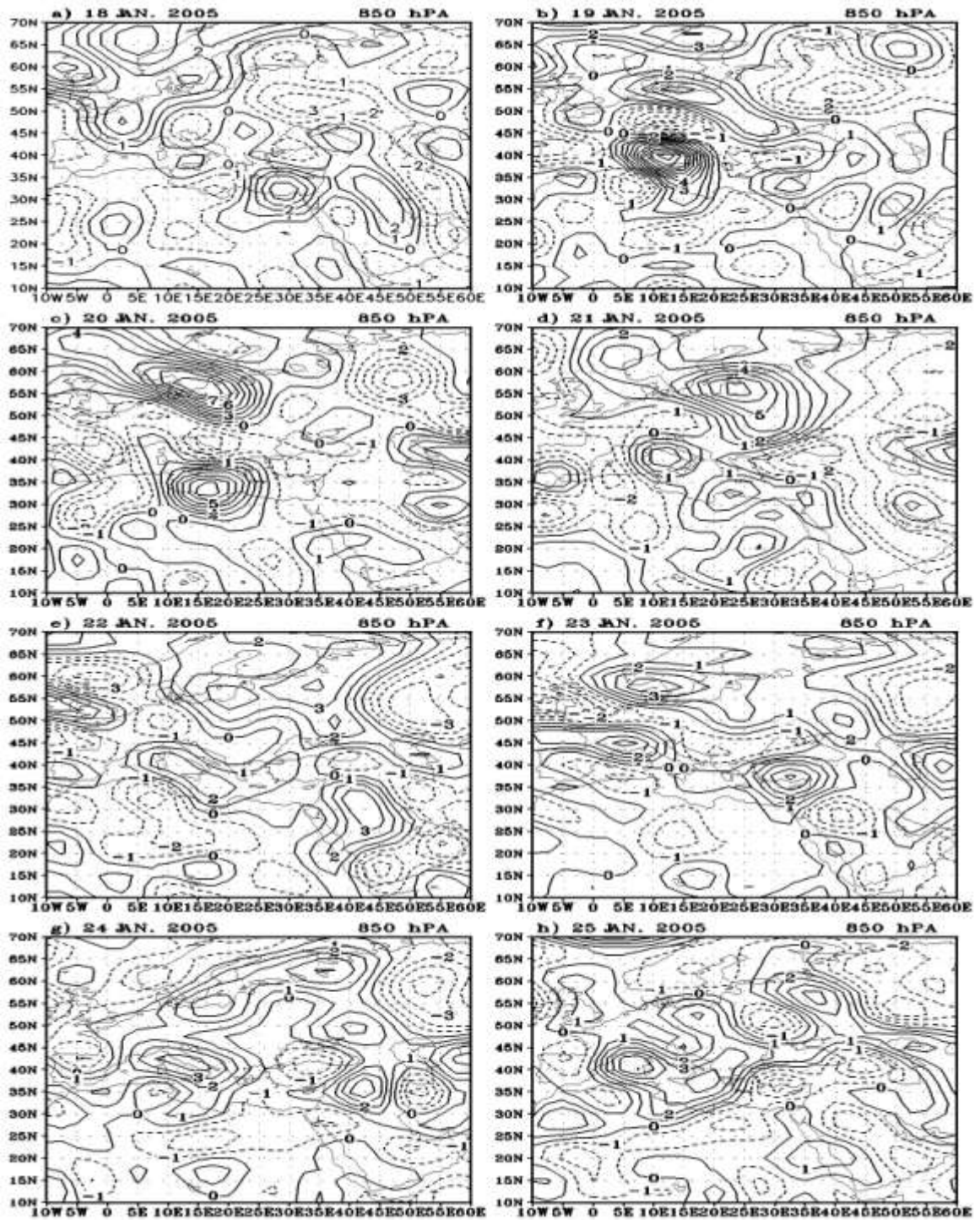


Fig. 5: Relative vorticity analysis at 850 hPa, contours every $1 \times 10^{-5} \text{ s}^{-1}$, (solid) lines denote positive values (dashed) lines denote negative values for 1200 UTC 18-25 January 2005.

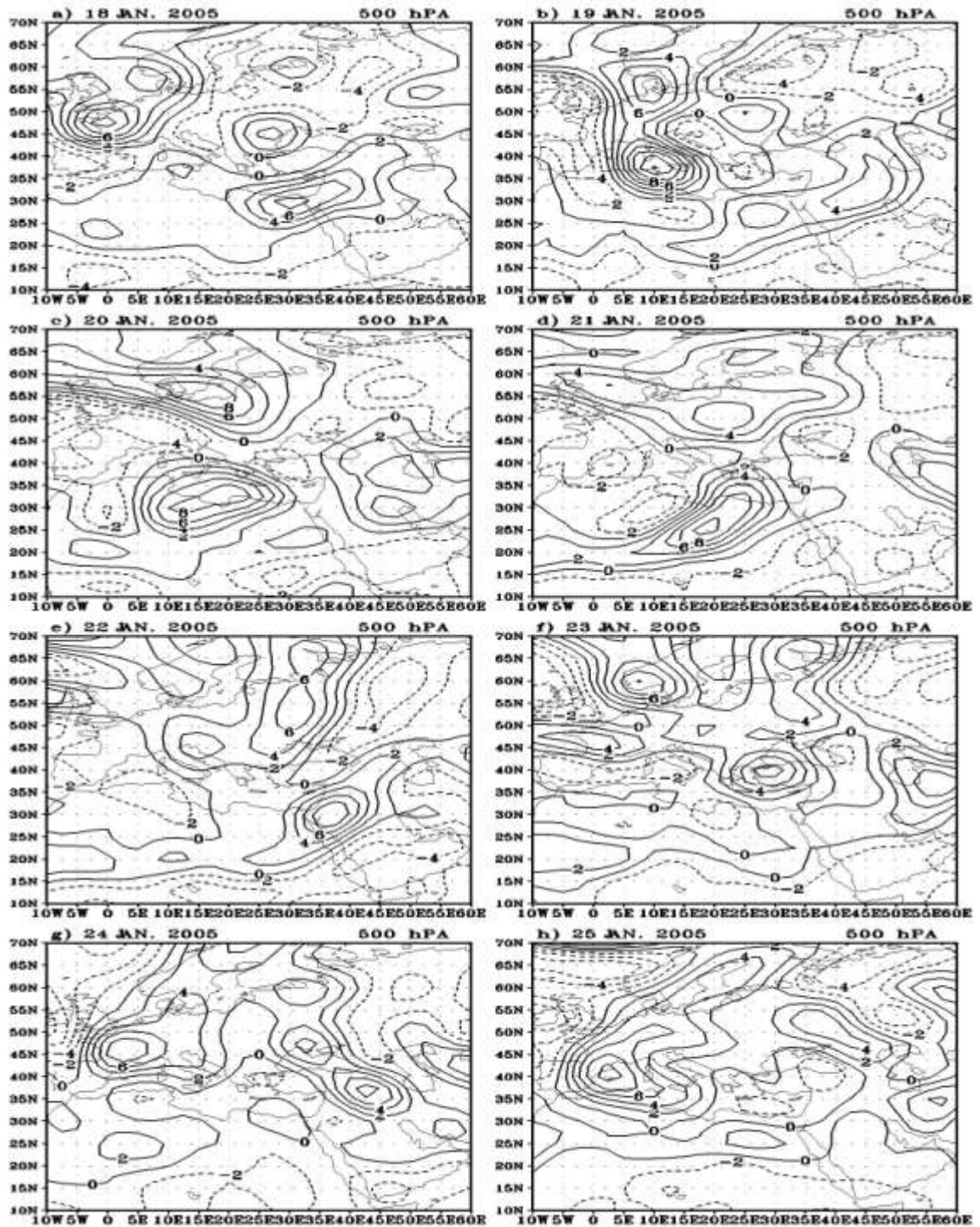


Fig. 6: Relative vorticity analysis at 500 hPa, contours every $1 \times 10^{-5} \text{ s}^{-1}$, (solid) lines denote positive values (dashed) lines denote negative values for 1200 UTC 18-25 January 2005.

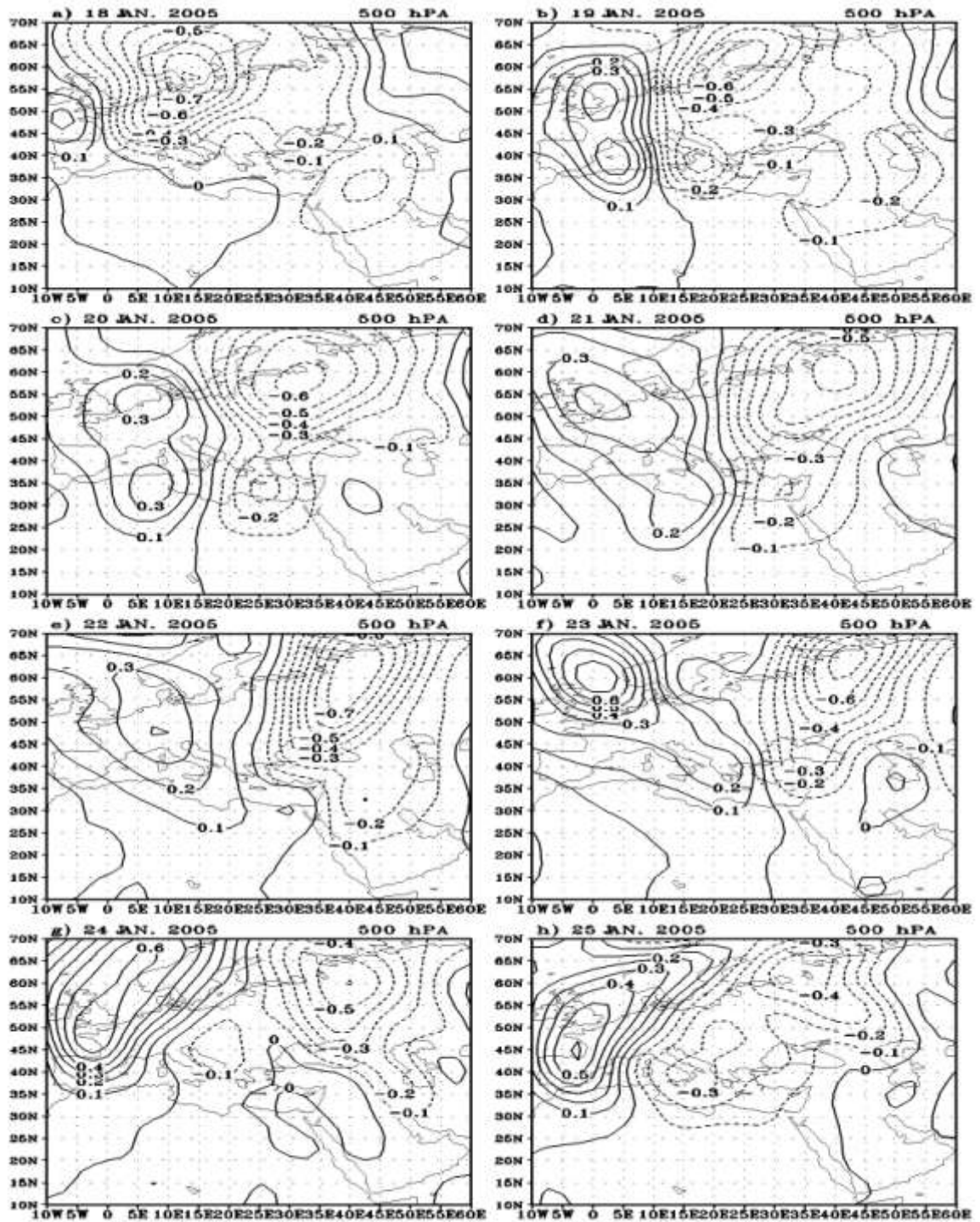


Fig. 7: Vertical motion analysis at 500 hPa contours every 0.1 Pa s^{-1} , (solid) lines denote positive values (dashed) lines denote negative values for 1200 UTC 18-25 January 2005.

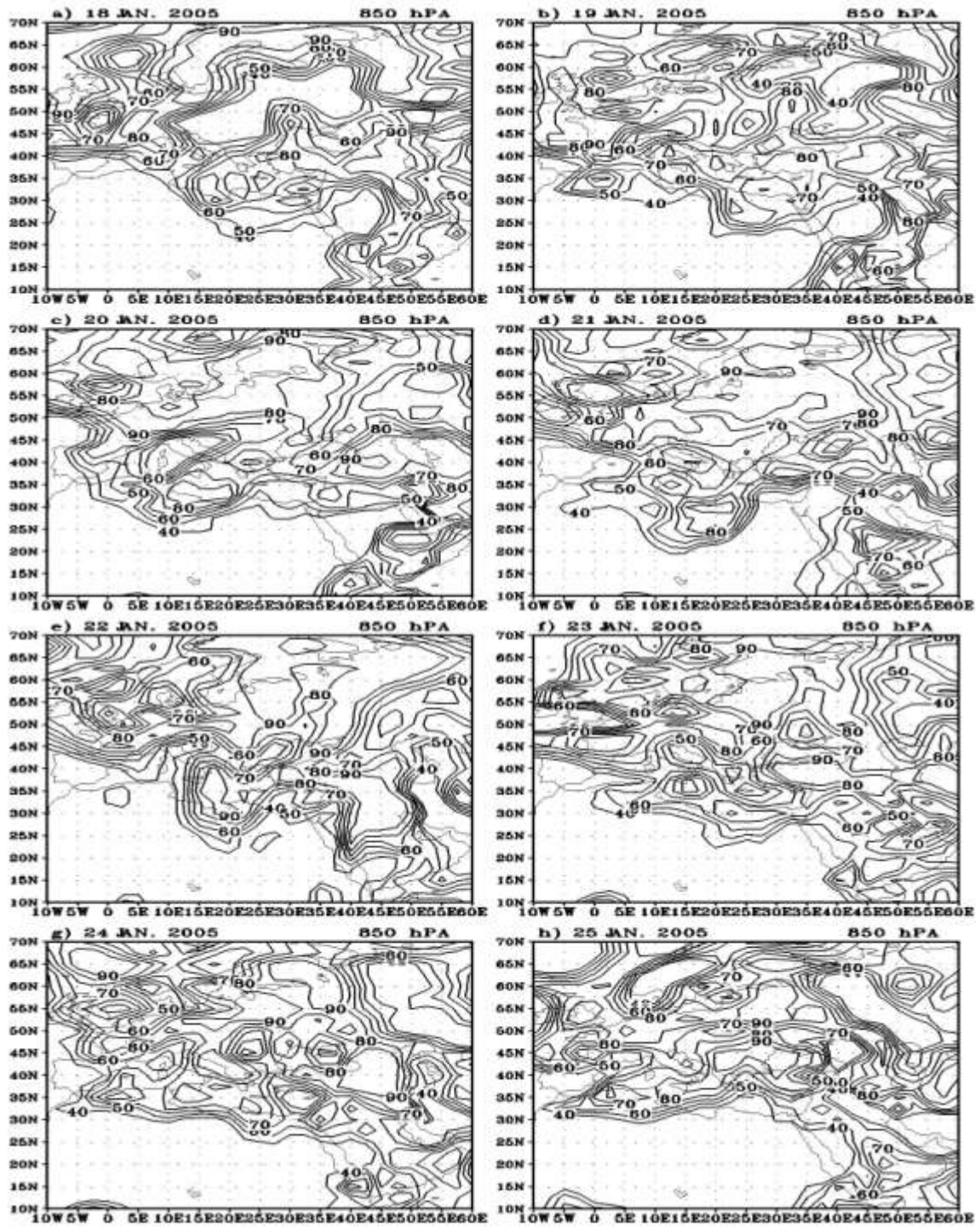


Fig. 8: Relative humidity objective analysis at 850 hPa, that $\geq 40\%$ isopleths every 10 % for 1200 UTC 18-25 January 1981.

longitude 20° E, figure 1d exhibiting a significant westward tilt with height, indicating a strong baroclinic atmospheric environment. The maximum value of relative vorticity is in excess of $10 \times 10^{-5} \text{ s}^{-1}$ figure 10d, while the absolute vorticity advection is maximized in the vicinity of the surface cyclone system, reaching $40 \times 10^{-10} \text{ s}^{-2}$. The ascent pattern had drifted eastwards over the same region, peaking at 0.8 Pa s^{-1} at 500 hPa (figure 8d) ahead of the surface system. A major factor allowing the surface low to convert available potential to kinetic energy is the advection of sinking cold air behind, and the advection of ascending warm air ahead of the low. This is especially evident at the 500 hPa isobaric level, in association with the vertical velocities chart figure 7d.

In the following 24 hours, the depression moved rather slowly, following the absolute vorticity advection maximum. As realized in figure 1e maximum development occurred at 22, when the surface system over east Europa connected and interact with the Sudan monsoon low over Red Sea air ahead of the low. This is especially evident at the 500 hPa isobaric level, in association with the vertical velocities chart figure 7d.

In the following 24 hours, the depression moved rather slowly, following the absolute vorticity advection maximum. As realized in figure 2e maximum development occurred at 22, when the surface system over east Europa connected and interact with the Sudan monsoon low over Red Sea KSA and northeast of Africa. The central pressure had dropped 20 hPa in 24 hours (not shown). Nevertheless, the closed system does not seem to satisfy the appropriate critical pressure rate in order to be classified as a bomb, according to Sanders and Gyakum (1980). By this time the maxima of vorticity and vorticity advection had weakened substantially figure 9e, that is the weakening of relative vorticity and absolute vorticity advection at 500 hPa had started before the surface pressure adopted its lowest value.

During 24 and 25 January the system became cut off at all the isobaric levels. It is noteworthy that the system started cut off at 500 hPa at 20 January, which is 24 hours after cyclogenesis had commenced. Its vertical tilt with height implies that it continued growing almost barotropically. The appropriate critical pressure rate in order to be classified as a bomb, according to Sanders and Gyakum (1980). By this time the maxima of vorticity and vorticity advection had weakened substantially figure 5e, that is the weakening of relative vorticity and absolute vorticity advection at 500 hPa had started before the surface pressure adopted its lowest value.

5. Potential vorticity analysis

In order to highlight the dynamical significance of the most important features that the synoptic overview and the relative vorticity analysis revealed, and to identify other distinct characteristics of the development, a (PV) analysis is carried out. In particular, the distributions of isentropic PV along with that of the potential temperature at the tropopause have been used to examine the upper level development. The low-level evolution has been investigated in terms of isobaric distribution of potential temperature and PV.

5.1 Upper level development

Figure 10 summarizes the evolution of the PV field on the 500 hPa isobaric surface from 18 to 25 January. Figure 10a displays three distinct anomalies: i) one of magnitude 3.5 PVU located northwest of England which represents and accompanies the cyclone of our interest, ii) one of magnitude 2.5 PVU that appeared north east of Mediterranean and iii) the third one is over northern Europe (60° N, 30° E). According to figure 14b, within 24 hours the first PV maximum (which is of our interest) propagated slightly southeastwards and its magnitude increases to 4.5 PVU while the second and the third become weakening. The important feature in figure 10b is that PV trough extended southwards up to north Algeria in the NW-SE direction. The larger scale dynamics are controlled by the presence of the polar jet stream on the western flank of the trough associated with intense PV gradients. On 20 January figure 10c, the main core of the PV trough located over central of Mediterranean, coinciding with the 500 hPa low-pressure center, which actually developed at the same time scale. The trough of PV extends in the NE-SW direction from northwest of Italy to west of Algeria, coinciding with the 500 hPa trough. An area of low PV values appeared ahead of the PV trough over east of Mediterranean. By 21 January the PV trough propagates southeastwards involving advection on its southern edge. The intensification of the winds resulted to the steepening of the PV gradients ahead of the trough, while the PV anomaly had reached the maximum value of 3.5 PVU (figure 10d). Also, it can be seen that the PV trough became more meridionally oriented at its southern edge.

By 22 January the trough had extended southerly and moved slowly eastwards to reach north of KSA. The PV gradients at its southern edge have increased significantly and originated over south east of Mediterranean and north of KSA and reached the maximum value of 3 PVU. It is interesting to note that this maximum is associated with a high values

of relative humidity, reaches to 90 % at 850 hPa and 75 % at 300 hPa, this is due to the area occurs in the area of ascending motion (Figures 7, 8). This time (22 January) represents the maximum propagation of the polar front jet stream southward and also the maximum amalgamation with the subtropical jet.

On the 23 January the PV trough moved northwest and extended latitudinally in association with the 500 hPa trough. As can be seen from figure 2g,h the low becomes stationary vortex rotating above the north east of Mediterranean, Also, the two coupling maximum of PV rotates with each other.

5.2 Lower level development

Figure 9 presents the PV analysis at 850 hPa for the period from 18 to 25 January 1981. Figure 9a displays two distinct anomalies, all to the southeast of the upper level anomaly: i) one of magnitude 1.3 PVU located northwest of England ii) one of magnitude 1.3 PVU northeast of Italy.

The first and second one of these anomalies are associated with values of relative humidity greater than 90 % (figure 8). It should be noted that the first one of these anomalies is the signature of the upper PV trough at the level of 850 hPa, imply that this anomalies are connected to stratospheric air, but rather originated at low levels. This was verified by examining in time each of the anomalies in relation to the PV trough. According to figure 9b, within 24 hours the first PV maximum propagated slightly southeastwards and it becomes located over northeast of England, the second one propagated southeastward.

On the 20 January, when the low-level wind pattern indicates a rapid intensification of the northerly and northwesterlies over north and west of Italy respectively figure 9c prior to the surface development, the first and second one of the low-level PV anomalies had propagated further to the south.

On the 21 January, as the dynamic support from the upper levels decreased figure 9d, the low levels appear to play more important role. The anomaly located at (40° N, 10° E) moved very fast to the southeast while the northern anomaly (55° N, 22.5° E) lies nearly northeast of this location. The first anomalies moved north ward while seem to be joined to a quite intense

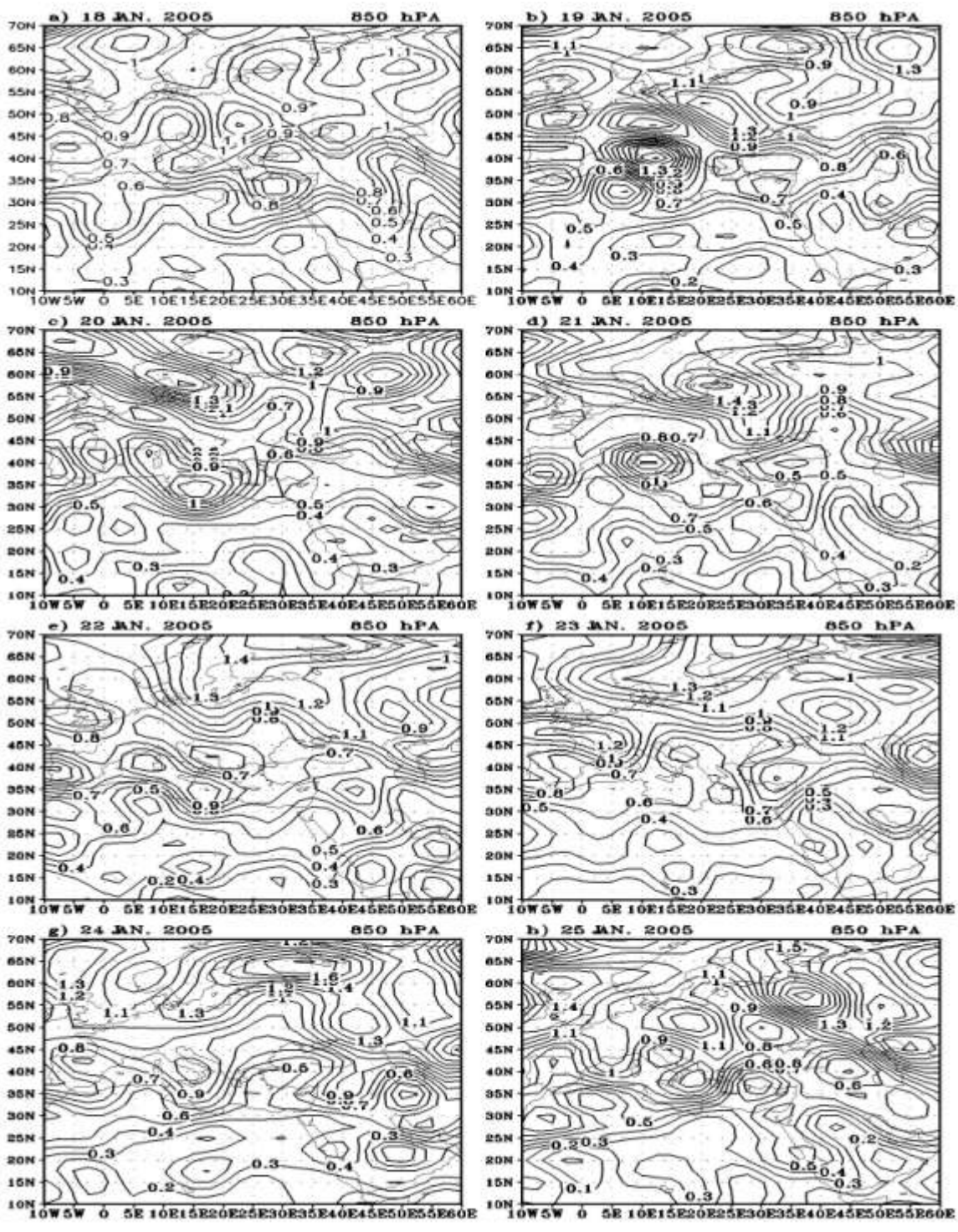


Fig. 9: Ertel's positive potential vorticity analysis at 850 hPa, that greater than or equal 0.5 PVU, contours every 0.1 PVU for 1200 UTC 18-25 January 2005.

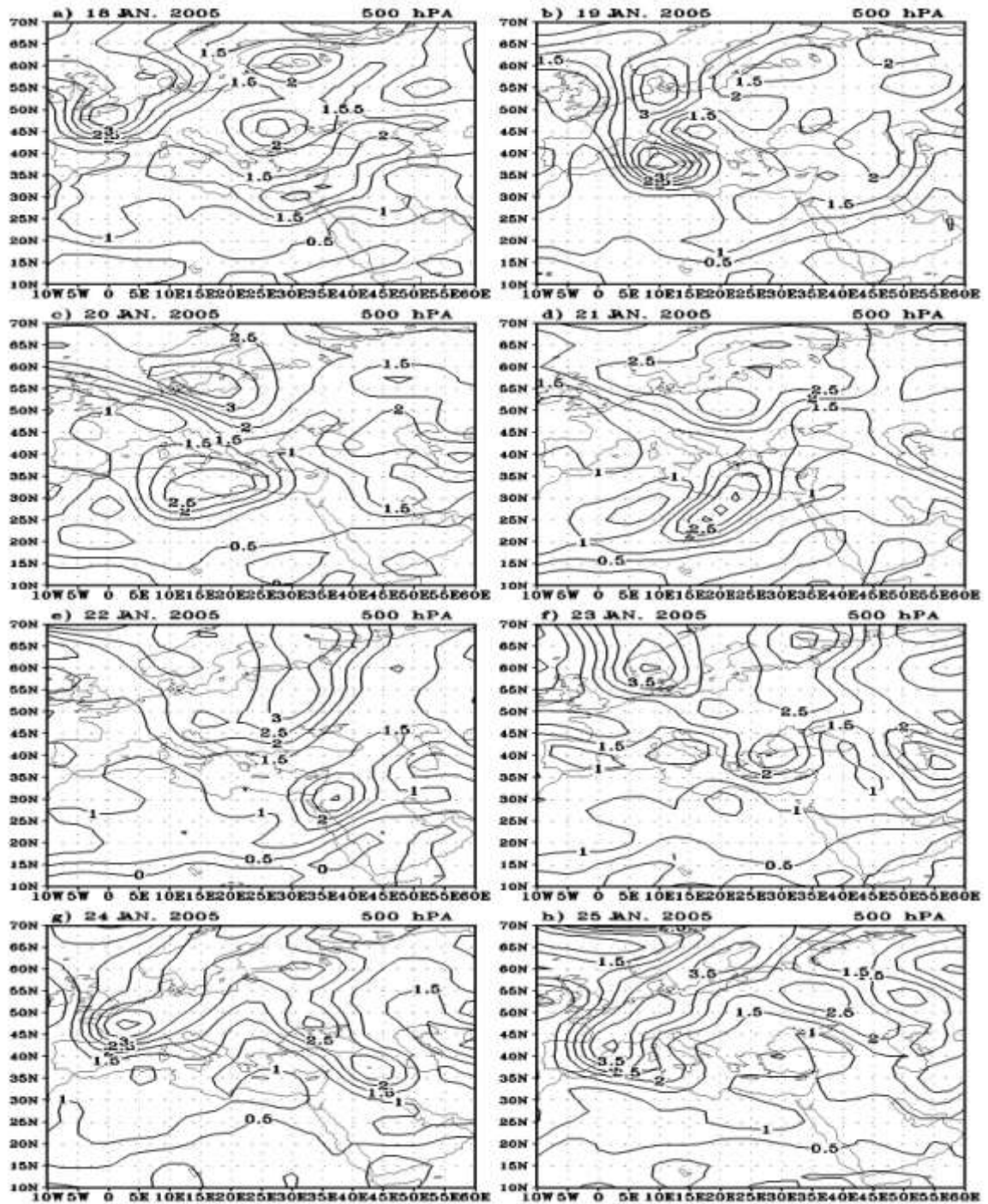


Fig. 10: Ertel's positive potential vorticity analysis at 500 hPa, that greater than or equal 0.5 PVU, contours every 0.1 PVU for 1200 UTC 18-25 January 2005.

low level anomaly over central Mediterranean and southeast of Italy, of magnitude 0.9 PVU. Just on the eastern flank of the upper level anomaly figure 10d this is accompanied

by a further increase of northeasterlies to 25 m s^{-1} (not shown). It is noteworthy that the low-level PV anomaly is situated almost under the area of the tropopause warm anomaly. According to Figure 9e, within 24 hours the PV maximum propagated southerly to reach the north coast of Libya and its value intensified to reach 1 PVU. At 23/ 12 where the system indicated cut off at all the isobaric levels, there is also a cut off of the PV anomaly and its values decreases to reach 0.8 PVU it moved to reach the northwest coast of Egypt. It decreases generally to reach its minimum values (0.6 PVU) with the end of the period (25 January) at the north of Egypt. The period is characterized by the area of PV anomalies is associated by values of relative humidity greater than 90% (figure 8).

6. Summary and conclusions

The dynamics of a case of cyclogenesis over the central and eastern Mediterranean, that occurred on 17- 28 January 2005, have been investigated in terms of two meteorological parameters: the isobaric absolute and relative vorticity and the isentropic potential vorticity. On the whole, the two approaches seem to identify the same features for surface cyclogenesis initiation in this case: the interaction of a region of positive absolute vorticity advection ahead of a 500 hPa trough with a shallow frontal system in the first approach, and an isobaric PV anomaly at the upper levels with a low-level baroclinic zone, (that is again with a shallow frontal system) in the second approach.

It is evident that, both analyses imply the significance of the upper level dynamics in the initiation of this case of cyclogenesis. On one hand, the isobaric vorticity analysis appears to be an informative, accurate and easy to use method for describing the upper-level dynamics. On the other hand the PV analysis provided a summarized picture of the development and the evolution at upper and lower levels, which is directly visible, on the basis of a smaller number of plots compared with the isobaric vorticity analysis. The display of the time sequence of the PV on the appropriate isentropic surface helped in easily understanding the dynamics of the three-dimensional upper level development.

The PV analysis identified possible effects at low levels in the central Mediterranean (where the positive lower PV anomaly resulted from the condensation of water vapor), an area where the diabatic processes appear to play an important role in cyclonic development. Nevertheless, this point requires further investigation to determine any of the above factors contribute to surface cyclogenesis, besides vorticity and warm

advection of course. Therefore, the PV analysis is recommended as a more convenient and comprehensive method for the interpretation of the dynamical mechanisms responsible for cyclogenesis over the central and eastern Mediterranean region, in relation to its particular characteristics due to the geographical location and topography of the Mediterranean basin.

Another feature that invites comment is the approach of the polar front and the subtropical jets over the central Mediterranean, resulting in the amplification of the upper-level winds, the deepening of the trough and the strengthening of the vorticity maximum over the central and eastern Mediterranean. Karein (1979), following Defant (1959), believes that this interaction can play a major role in the central and eastern Mediterranean cyclogenesis during cold seasons.

References

- Carlson, T.S., 1991: *Mid - Latitude Weather Systems*. Harper Collins Academic. New York, 507pp.
- Defant, F., 1959: On the hydrodynamic instability caused by approach of subtropical and polar front jet stream in northern latitudes before the onset of strong cyclogenesis. In: *Rossby Memorial Volume: The atmosphere and sea in motion*. B. Bolin (Ed.), Rockefeller Inst, New York, pp 305-325.
- Ertel, H., 1942: Ein neuer hydrodynamischer Wirbelsatz. *Meteor. Z.*, **59**, 277-281.
- Flocas, H.A and T.S. Karacostas., 1996: Cyclogenesis over the Aegean sea: Identification and Synoptic Categories. *Meteorol. Appl.*, **33**, 53-61.
- Holton, J. R. 1979: *An introduction to Dynamic Meteorology*. Academic Press, New York, 391pp.
- Hoskins, B. J., M. E. McIntyre, and A. W. Robertson.,1985: On the use and significance of isentropic potential vorticity maps. *Quart. J. Roy. Meteor. Soc.*, **111**, 877-946.
- Karacostas, T.S. and A.A. Flocas., 1983: The Development of the Bomb over the Mediterranean area. *La Meteorologie*, **34**, 351-358.
- Karein, A.D., 1979: The Forecasting of Cyclogenesis in the Mediterranean Region. Ph.D. Thesis, University of Edinburgh, Scotland, 159pp.
- Krisnamurti , T. N., and L. Bounoua, 1996: *An introduction to Numerical Weather prediction Techniques*. Academic press, pp. 73-76.
- Kurz,M., 1994: The role of diagnostic tools in modern weather forecasting. *Meteorol. Appl.*, **1**, 45-67.
- Palmen, E. and C. Newton., 1969: *Atmospheric Circulation Systems: Their structure and Physical interpretation*. New York and London. Academic Press. 603 pp.
- Petterssen, S., 1956: *Weather Analysis and Forecasting*. Vol. 1, Mc Graw- Hill Book Company, 2nd

Ed. New York, 428 pp.

Prezerakos, N.G., 1991: Formation of Sub-synoptic-scale waves on the eastern flank of a large anticyclone at 500 hPa leading to surface cyclogenesis in the Greek area on 5th October 1989. Report on the fourth session of the steering group on Mediterranean Cyclones study project. WMO/TD No. 420. pp. 99-110.

_____, N.G., 1992: Some appreciable tropospheric circulation features leading to surface cyclogenesis in the central Mediterranean region. Extended Abstracts of Papers ICS/ICTP/WMO International Workshop on Mediterranean Cyclones Studies, International Center for Theoretical Physics, Trieste, Italy, 18022 May, pp. 74-80.

_____, N.G., Flocas, A. H. and S.C Michaelides, 1999: Upper – tropospheric downstream development leading to surface cyclogenesis in the central Mediterranean. *Meteorol. Appl.*, **6**, 313-322.

Rossby, C. G., 1940: Planetary flow patterns in the atmosphere. *Quart. J. Roy. Meteor. Soc.*, **66**, 68-87.

Sanders, F. and J.K. Gyakum., 1980: Synoptic-Dynamic Climatology of the Bombs. *Mon. Wea. Rev.*, **108**. 1589-1606.

Wiin-Nielsen, A. 1973: Dynamic Meteorology. WMO-No. 364, Geneva, 367pp.

WMO, 1986: Atmospheric ozone, Vol. I. Report No. 16. Geneva: WMO, 264pp.

العلاقة بين الدردورية الجهدية وتكون وتطور المنخفضات
On the relationship between Potential Vorticity and Cyclogenesis

د. عبد الرحمن خلف الخلف

كلية الأرصاد والبيئة وزراعة المناطق الجافة - جامعة الملك عبد العزيز
 جدة - المملكة العربية السعودية

ملخص البحث:

تعتبر المنخفضات والمرتفعات الجوية هي المقياس السينوبتيكى المسيطر لأنظمة الطقس الجوية في مناطق العروض الوسطى. ومن الطرق الجذابة والعملية لدراسة المفاهيم الديناميكية لهذه الأنظمة الضغطية استخدام الإطار العلمي للدردورية الجهدية. وفي هذا البحث تم بحث مفاهيم عديدة لتكون المنخفضات وتطورها في منطقة العروض الوسطى باستخدام هذا الإطار للدردورية الجهدية من خلال دراسة وتحليل منخفض جوى. اتضح من تحليل الدردورية الجهدية المطلقة والنسبية أهمية العمليات الديناميكية في المستويات العليا لبدء عملية تكون وتطور المنخفض. واتضح أن تحليل الدردورية على المستويات الضغطية المختلفة يعطى سهولة ودقة وكم من المعلومات المفيدة لوصف ما يحدث في طبقات الجو العليا ديناميكيا. ومن ثم فان تحليل الدردورية الجهدية قدم صورة متكاملة لنمو وتطور المنخفض على المستويات العلوية والسفلية. وقد ساعد استنتاج وعرض الدردورية الجهدية مع الزمن على مستوى ايزنتروبيكى مناسب على سهولة فهم ديناميكية تكون وتطور المنخفض على المستويات العليا وفي الأبعاد الثلاثية.